

Fluorenyl Based Syndiotactic Specific Metallocene Catalysts Structural Features, Origin of Syndiospecificity

Abbas Razavi,*¹ Vincenzo Bellia,¹ Yves De Brauwer,¹ Kai Hortmann,¹ Liliane Peters,¹ Sabine Sirole,¹ Stephan Van Belle,¹ Ulf Thewalt²

¹ Atofina Research S.A., Centre de Recherche Du Groupe Total, Zone Industrielle C, B-7181 Seneffe (Feluy), Belgium

² Sektion für Röntgen und Elektronenbeugung Universität Ulm, Germany

E-mail: abbas.razavi@atofina.com

Summary: The stereochemistry of propylene insertion/propagation reactions with a variety of C_s symmetric fluorenyl- containing single site catalysts is discussed. Our recent results indicate that independent of the chemical composition of the ancillary ligand fragments, or nature of the transition metal, active sites with local C_s symmetry and enantiotopic coordination positions behave syndiospecifically in the general context of chain migratory insertion mechanism. Perfect bilateral symmetry neither exists nor is required in these processes. In this context the mechanism of syndiospecific polymerization is revisited by taking into account the structural characteristics and catalytic behavior of the original metallocene based (η^5 -C₅H₄-CMe₂- η^5 -C₁₃H₈) MCl₂/MAO; M = Zr (1), Hf (2) catalyst systems and new syndiotactic specific systems including (η^5 -C₅H₄-CPh₂- η^5 -3,6-di-tBut-C₁₃H₆)ZrCl₂ (3), η^1, η^5 -(μ -Me₂Si)(3,6-di-tBut-Flu)(t-ButN)MCl₂/MAO; M = Ti (4), Zr (5) and η^1, η^5 -(μ -Me₂Si)(2,7-di-tBut-Flu)(t-ButN)MCl₂/MAO; M = Ti (6), Zr (7).

Keywords: catalysis; mechanism; metallocene; polypropylene; syndiospecificity

Introduction

Syndiotactic polypropylene was first isolated by Natta and his co-workers as a minor by-product of isotactic polypropylene produced with a TiCl₃ based catalyst.^[1] The nature of the active site and the mechanism of formation of this polymer are still under debate. It is believed that it is formed on the sites with low chlorine coordination via a chain end controlled mechanism. Later Zambelli and coworkers produced syndiotactic polypropylene directly using a vanadium-based homogenous catalyst.^[2] In this case, more is known about the nature of the active site and the mechanism of the polymerization is elucidated

satisfactorily. No X-ray structure of the catalyst precursor is, however, available due to its very temperature sensitive nature. After the discovery of the bridged cyclopentadienyl-fluorenyl metallocene based syndiospecific catalyst and the resulting syndiotactic polypropylene by us^[3] one had for the first time the opportunity to make accurate statements about the nature of the active site and the mechanism of the polymerization. By studying the available X-ray structure data of the metallocenes and their stabilized alkylmetallocenium cation^[3h] it has become possible to make reasonable deductions on the nature of the active site and its behavior during the polymerization. The concept of active site model and the mechanism of the polymerization have been refined gradually and continuously as new syndiotactic specific metallocenes were discovered and more elaborate calculation methods were applied. In this contribution we report the latest progress on catalysts development and mechanistic aspects of syndiospecific polymerization commencing with a review of the original model proposed for the isopropylidene (cyclopentadienyl-fluorenyl)MCl₂ / MAO; M = Hf, Zr catalyst systems.

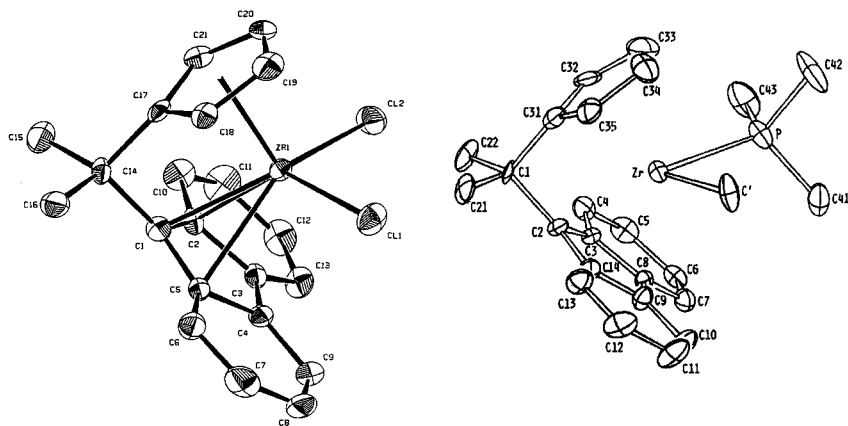


Figure 1. X-ray determined molecular structure of **1** (left) and its trimethyl phosphine stabilized methylmetallocenium cation (right).^[3h]

Results and Discussion

Figure 1 presents the X-ray determined, molecular structure of the metallocenes

polymerization. This depiction is based on the relative importance of the non-bonded, steric interactions operating on different parts of the catalytic species and its - in the polymerization active participants - aromatic ligand, polymer chain and the coordinating monomer in the following order.

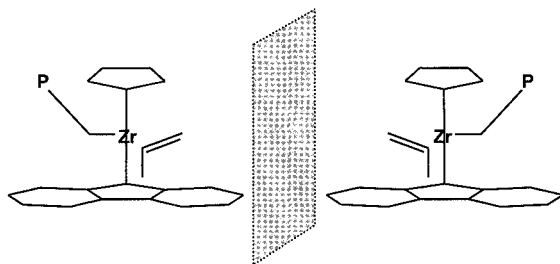
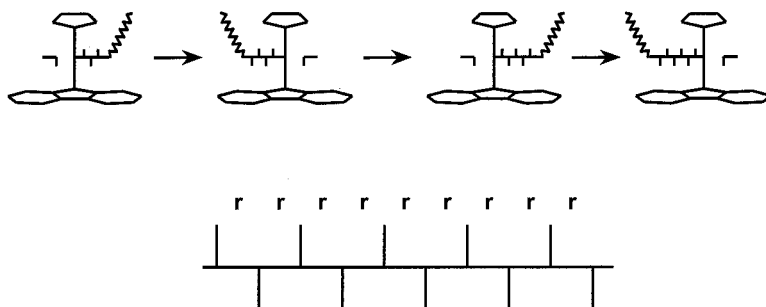


Figure 2. Interconverting, mirror image related active species produced with **1**.

The steric interaction between the flat and spatially extended fluorenyl ligand forces the growing polymer chain to be oriented towards the free space left (or right) to the unsubstituted cyclopentadienyl moiety of the ligand. To avoid excessive steric exposure, the incoming approaches with its methyl group trans to the growing polymer chain. The system reaches in this way a minimum energy state. In this orientation the coordinated monomer points with its methyl group head-down into the empty space in the central region of the fluorenyl ligand. The confirmation for the head-down coordination of the monomer was determined after extensive molecular mechanics and force field calculations performed by Corradini and coworkers.^[4] The model underwent later additional refinement and took its current form after experiments conducted by several groups^[5] supporting the idea of an α C-H agostic assistance in the transition state for the propylene polymerization.



Scheme 1. Mechanism of syndiospecific polymerization (top). Fischer projection of an ideal syndiotactic chain (bottom).

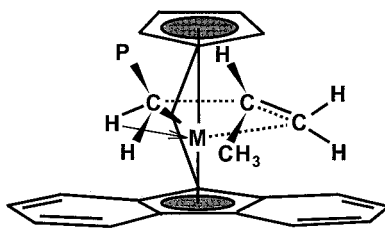


Figure 3. Transition state structure proposed based on the X-ray structures given in Figure 1.

The working hypotheses, active site model and the transition state structure discussed in the preceding paragraphs, account for syndiotactic specificity of the catalysts and formation of the syndiotactic polypropylene chains. Additionally, this justifies the formation of microstructural stereo errors - the meso triad (mm) and meso dyad (m) defects - encountered in the backbone of the polymers. The former – the so-called enantiomorphic site controlled defects - are well described and relate to reverse monomer enantioface insertion. The origin of the temperature and monomer concentration dependent m type stereo error, is more complex and more difficult to discern. Their formation has been explained according to the insertion-less site epimerization scheme shown in Figure 4.

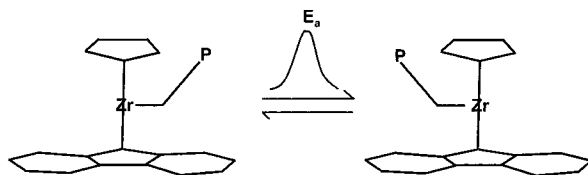


Figure 4. Coordination sites' equivalency and endothermic active site epimerization.

The R and S configured active sites are equi-energetic (Figure 4) and therefore may interconvert during the polymerization. The interconversion is particularly enhanced, in the absence of a coordinating monomers or solvent molecules. If the rate of this interconversion is faster than the actual rate of the monomer insertion, sites epimerize before the next insertion occurs. This increases the chance of two consecutive insertions taking place at the same enantiomorphic coordination position thus, adding two monomer units with the same prochiral face. This leads to the formation of meso dyad defects within predominantly syndio-regular polymer backbone. Even though the interconverting species are equi-energetic, the site epimerization requires activation energy for the chain's back or forth swing. The concept of site epimerization is, in principle, very close to the mechanism of chain back migration proposed by Cossee and Arlman in 1964.^[6] The close proximity of a polar molecule, a counter ion, and/or temporarily blockage of one of the coordination sites (contact ion pairing) can provoke the site epimerization by favoring the polymer chain to move away and migrate back to its initial position. We have suspected this mechanism to be the cause for the formation of the short isotactic blocks that were detected in the backbone of the predominantly syndiotactic polymer chains formed with **2** (Figure 5).

It is conceivable that the MAO anion as counter ion, occupies the very same spot where the trimethyl phosphine is located in the structure shown in Figure 1 left. Under these conditions, its polarity and size would discourage the chain from moving to that position and provoke multiple insertions at the same coordination site, before the counter ion dissociates and regular chain migratory insertion process kicks in again. The occurrence of the site epimerization can be easily demonstrated and manipulated via polymerization temperature

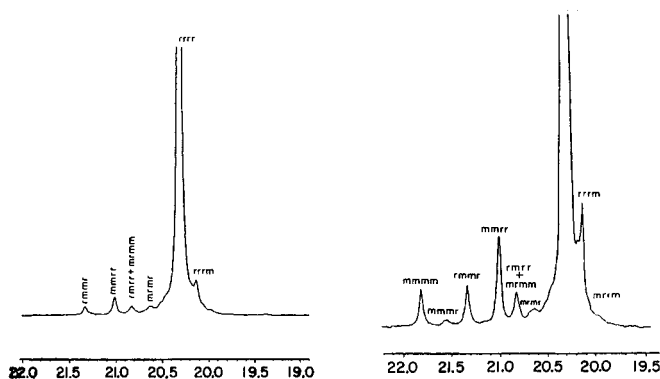


Figure 5. The methyl region of ^{13}C NMR of syndiotactic polypropylene produced by **1** (left) and **2** (right).^[37]

and monomer concentration modifications and also by distorting the coordination sites' equivalency. By playing with these parameters, the isotactic sequence lengths in predominantly syndiotactic polymers have been enlarged, to the extreme cases, where "pure" isotactic polymer chains were obtained.^[7, 8]

To decrease the *rmrr* concentration (increase the overall stereoregularity of the syndiotactic polypropylene) we should lower the site epimerization rate to greatest possible extent. One way to accomplish this goal is to perform the polymerization in liquid propylene (high monomer concentration) at lowest possible temperatures. Of practical interest is, however, to accomplish this goal through structural modifications and/or by playing with the counter ion composition/interaction. The structure/counter ion modification which not only helps lower the frequency of *rmrr* stereodefects but also enhances the enantioselectivity of the catalysts (*vide infra*), can have an additional benefit in lowering the concentration of the *rmrr* pentads.^[9b, 3g] Figure 6 illustrates the X-ray determined molecular structure of $(\eta^5\text{-C}_5\text{H}_4\text{-CPh}_2\text{-}\eta^5\text{-3,6-di-tBut-C}_{13}\text{H}_6)\text{ZrCl}_2$ (**3**). After activation, complex **3** polymerizes propylene to highly stereo-regular polypropylene very efficiently, especially in the presence of hydrogen. Table 1 presents the polymerization results and polymer analysis of the syndiotactic polymers produced with catalyst system **3**/MAO, at different polymerization temperatures. Table 2 compares the meso dyad and triad concentrations found in syndiotactic polymer chains

produced with metallocene **1** and **3**. A cursory glance at the data given in Tables 1 and 2 reveals that the *t*-butyl substitution in positions 3 and 6 of the fluorenyl moiety of the ligand in metallocene **1** causes substantial improvement in stereoselectivity of the final catalysts. It decreases the concentration of both meso dyad and triad related stereoerrors.

Table 1. Polymerization results and polymer analysis for **3**/MAO catalysts system

Temperature °C	Mw	rrrr %	Regiodefects %	<i>T_m</i> °C
40	766,000	91	nd	150
60	509,000	88.5	nd	143
80	443,000	79	nd	128

For example, the rmrr pentad concentrations in syndiotactic polymer chains produced with **3** are, by about 1/3, lower than that of the corresponding pentad concentrations in polymers made with **1**/MAO catalyst system. They double in size, in both systems, with every 20°C increase in polymerization temperature. On the other hand, the rmmr pentad concentrations in polymers produced with **3** are about half of the corresponding pentad concentrations observed in polymers made with **1**/MAO and vary little with temperature. The improved enantioselectivity (lower rmmr %) of catalyst **3**/MAO can be reasonably explained, by the enhanced substituent(s) effect in directing the polymer chain, to adopt the most preferred upward conformation - left or right to the cyclopentadienyl moiety. This provides a more effective guidance for the monomer's head down coordination mode (tighter "chiral pocket"). The explanation for lower rmrr pentads concentrations in polymers produced with **3**/MAO catalyst system, at the same polymerization temperatures and monomer concentrations, is however, less straightforward. It could be related to different cation/anion interaction mode for **3** and **1**.

Table 2. Stereo defects generated in the polymers produced with **3** (left) and **1** (right)

Temperature °C	rmmr %	rmrr %	rmmr %	rmrr %
40	0.73	0.93	1.55	1.15
60	0.85	1.99	1.65	2.7
80	1.06	3.79	2.20	4.82

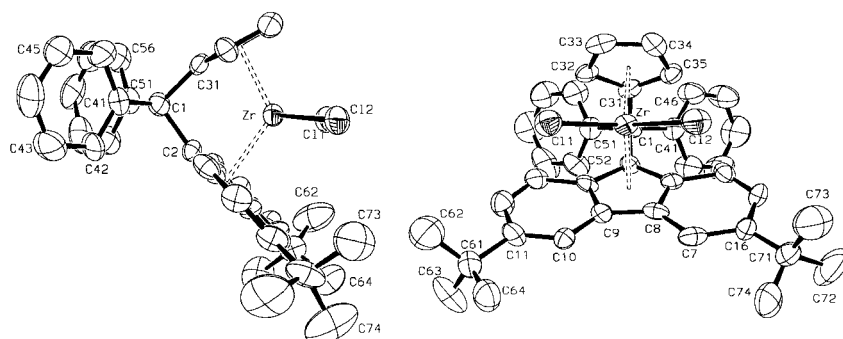


Figure 6. Side and front view perspectives of X-ray determined molecular structure of **3**.

A cursory check of the front view of the molecule **3** shown in Figure 6 and simple modeling experiments suggests that the spatial extension of the *t*-butyl groups can cause substantial steric interaction between the *t*-butyl substituents and MAO counter ion and the build up of strong repulsive forces against the formation of contact ion-pairs between metallocenium-methyl cations of **3** and anionic MAO molecules. Consequently, this could lower the site epimerization rate and the frequency of single *m* dyad formation.

We have recently reported two interesting syndiospecific cases for which similar substituent effects have been observed.^[10] These new syndiospecific catalyst systems are composed of the amido complexes, $\eta^1, \eta^5-(\mu\text{Me}_2\text{Si})(3,6\text{-di-}t\text{But-Flu})(t\text{-ButN})\text{MCl}_2$; $\text{M} = \text{Ti}$ (**4**), Zr (**5**) and $\eta^1, \eta^5-(\mu\text{Me}_2\text{Si})(2,7\text{-di-}t\text{But-Flu})(t\text{-ButN})\text{MCl}_2$; $\text{M} = \text{Ti}$ (**6**), Zr (**7**). After activation with MAO both Ti complexes (**4** and **6**) polymerize propylene to high molecular weight syndiotactic polypropylene, very efficiently. Conversely, the corresponding Zr homologues (**5** and **7**) give rise only to low molecular weight oligomers.^[11] The polymerization results and some polymer properties of syndiotactic polypropylene produced with **4** and **6** are summarized in Table 3. The degree of stereoregularity of the polymers, produced at different polymerization temperatures, measured as the concentration of *rrmmr* and *rmrr* pentads concentrations, is given in Table 4. The data presented in Tables 3 and 4 reveal that the stereoselectivity of both catalyst systems is higher than one would expect from catalyst systems with such flexible, low stereoridity, precursor structures. Under more favorable conditions, in liquid monomer

Table 3. Polymerization results and polymer properties of **4**/MAO catalyst system

Temperature °C	Mw	rrrr %	Regiodefects %	<i>T_m</i> °C
40	>1000,000	81.6	nd	123
60	765,000	74.8	nd	105
80	703,000	69.4	nd	98

and comparatively low temperature ($T < 30^{\circ}\text{C}$), the catalysts are even more selective. More recent investigations revealed that the polymers of **4** show quasi-perfect stereoregularity.^[11b] The remaining few stereo defects are mostly related to mm-type errors arising from occasional reverse monomer enantio face selection. The stereoregularity, however, suffers with decreasing monomer concentration and/or increasing polymerization temperature, mainly as a result of an increased probability of consecutive monomer insertion at the same enantiomorphic coordination position (site epimerization) with the corresponding formation of m-type stereodefects. Since in the chain end control mechanism the formation of m defects is independent of monomer concentration, the monomer concentration dependency of rmmr pentads can be taken as the key clue for the correct interpretation of the polymerization mechanism.^[11b,e,f]

Table 4. Stereodefects formed with **4** (left) and **6** (right) at different temperatures.

Temperature °C	rmmr %	rmrr %	rmmr %	rmrr %
40	1.49	3.37	1.55	4.80
60	1.73	6.45	3.03	8.55
80	1.75	8.34	8.00	11.20

The t-butyl substitution in positions 3 and 6 of the fluorenyl, brings about a much more dramatic improvement both with respect to stereo- and enantioselectivity than similar substitution in positions 2 and 7. The enantioselectivity of **4**, measured as the concentration of rmmr pentads, is higher than **6** and is close to the corresponding pentad values of **1** (Cf Table 2). Similarly, the rmmr pentad concentrations in polymers produced with **4** do not vary much with polymerization temperature. However, the overall stereoselectivity of **4** decreases much faster compared to **1** with increasing polymerization temperature due to a much sharper

increase in rmrr pentad concentrations. For polymers produced with **6**, the temperature effect, with respect to both enantio- and stereoselectivity, is even more dramatic. At 40 °C the polymers of **6** exhibit almost the same level of rmrr pentads as is found in polymers produced with **4** (1.55 vs. 1.49). However, at 60°C they double in size (3.03 %) and reach the 8% level (1.75% for **4**) at 80°C. On the other hand, the site epimerization related pentads, rmrr, for **6** are about 30% higher than the corresponding rmrr pentad concentrations for polymers produced with **4** at 40 °C. They double in both cases at 60°C and reach the staggering value of over 11 % for **6**.

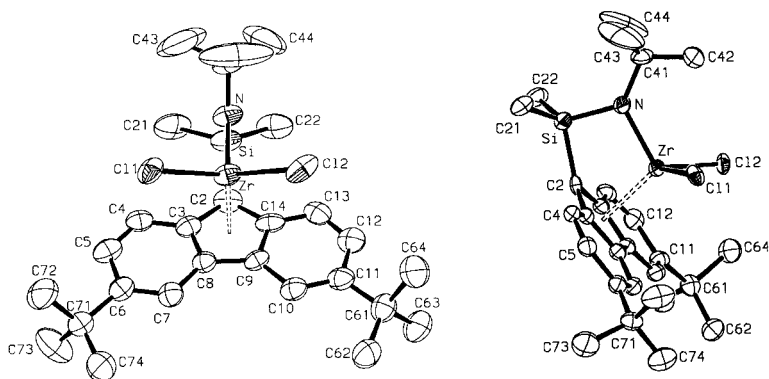


Figure 7. Front and side view perspectives of the X-ray determined structure of the **5** (**4**).^[10a]

Figure 7 depicts two different views of the X-ray determined molecular structure of **5**. Similar structure has been recently determined for **4**. It reveals the most important structural features of the metallocene precatalysts, which is, for lower part of the molecules, very close to the structural properties of molecule **3** shown in Figure 6. Therefore similar improved stereoregulating behavior, like in the case of **3**, due to the substituents' steric interaction with the counter-ion(s), is expected and observed. Structures **4** and **6** are the only fully characterized examples of syndiotactic specific structures that have titanium as active transition metal and produce high molecular weight syndiotactic polymer chains. They are also in many other aspects different from the original syndiotactic specific systems. They

consist of half sandwich molecules, contain amido type N-Ti (or Zr-N) bonds, and are 12 electron systems (14 electron systems at the most if one considers the participation of the lone pair electrons on the nitrogen to N-Ti bond). This leaves 10 (maximum 12) electrons only for the cationic active species. The most important difference between structure of **1** and **4** is, however, related to their stereo rigidity. Structure **4** (and also **6**), contains only one aromatic penta-hapto bonded ligand and possesses much lower stereo rigidity, yet it produces highly stereoregular syndiotactic polymers.

Concluding Remarks

The original model described in the “results and discussion” section including the chain migratory insertion mechanism explains the formation of syndiotactic polymer chains with a prochiral metallocene structure with bilateral symmetry. According to Scheme 1, the regularly alternating enantiofacial preference for monomer, at two enantiotopic coordination positions of the active site is the main characteristic of syndiospecific polymerization of propylene with C_s symmetric catalyst systems. Despite its simplicity and convenience the model has some handicaps. It is conceived of images coming from X-ray analysis performed on molecules contained in crystalline lattice in solid state and developed by force field calculations. It considers only frozen images of dynamic molecules and reflects only one aspect, the general shape and outline of the rigid molecules. These images reflect only a snapshot of the constantly vibrating, bending, “breathing” and freely floating molecules. The model disregards completely the dynamic nature of the active species and interactions of the counter-ion molecules and involved ion-pair association/dissociation equilibrium. Recent more flexible structures like **4** and **6**, structures with lower symmetry,^[13] ^{13}C -NMR / ^1H -NMR data of the original syndiotactic specific structures, and their chemistry are all indicative of haptotropic and fluxional nature of the metallocene molecules during polymerization.^[12d]

These “details” have often been neglected for the sake of simplicity and to prove their existence and impact has not been easy. However, one should be aware that at least two dynamic phenomena are actively involved, in one way or the other, in different steps of the polymerization and influence its mechanism, in one or the other direction. For example, the phenomenon of hapticity change or variation of bond order, between the transition metal and the aromatic ligands, should be seriously considered as being involved in certain metallocene

catalysts as we have demonstrated.^[12]

The haptotropy and ring slippage (Figure 8) can influence the instant electronic properties of the active site, the steric environment of its surrounding and impact the molecular weight and tacticity of their polymers. The second phenomenon is related to geometric change of the active species during the coordination and insertion steps. The pseudo tetrahedral geometry, which is assumed for the tetra-coordinated transition metal in the transition state, cannot be further extended to the geometry of the site in the step just after the insertion. At this stage the

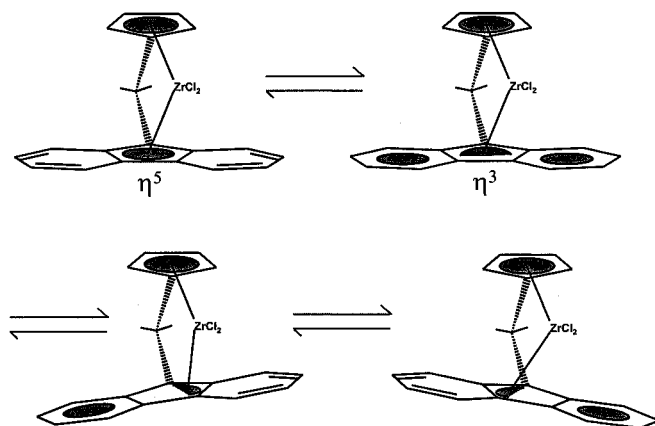


Figure 8. Fluorenyl bond haptotropy and ring slippage.

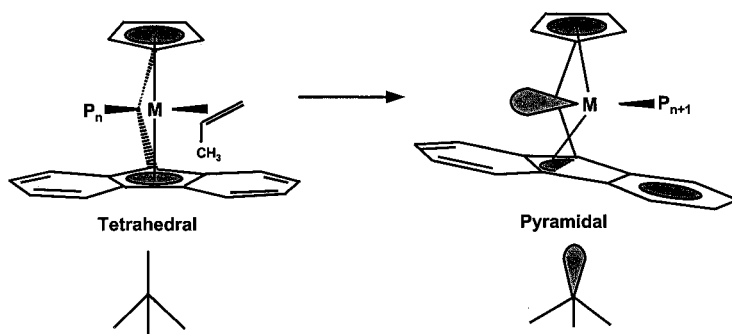


Figure 9. Systematic structural change and geometry variation during the insertion steps.

tetra-coordinated structure collapses, due to the disappearance of a ligands, leaving a tri-coordinated species behind in which the repulsive forces, acting upon the bonding electron pairs, are different and require a new geometry. The most logical structure that can be suggested for this step would be a trigonal pyramid (Figure 9 right). After the next monomer coordination, again the structure will adopt a tetrahedral geometry (Figure 9 left). This change in geometry, operating on all alkyl metallocenium cations, is probably of more importance for the syndiospecific case, where dynamic processes, such as chain migration and site epimerization (vide supra), are vital for its existence. Finally, another ligand/transition metal related dynamic behavior that can be envisaged to be acting on the transition structure is the lateral semi-rotational displacement of the whole ligand system around the transition metal (or vice versa) reported by Petersen^[14] is also noteworthy in this context. This movement that can be described as a kind of wind shield wiper type oscillation of the metalacyclobutane moiety within the “fixed” ligand system might have a facilitating effect on the site epimerization and/or chain migration mechanisms. Especially in C_1 symmetric systems (Figure 10).

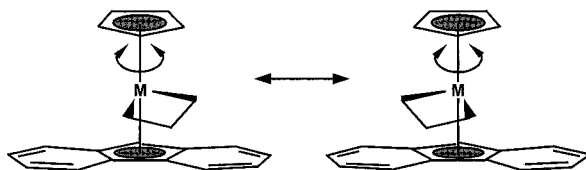


Figure 10. Lateral displacement of ligand system around the centroids-Zr bond axis (the bridge is omitted for the sake of clarity).

- [1] [1a] G. Natta, I. Pasquon, P. Corradini, M. Peraldo, M. Pegoraro, A. Zambelli, *Rend. Accad. Naz. Lincei*, (8), **1960**, 28, 539; [1b] G. Natta, I. Pasquon, P. Corradini, M. Peraldo, M. Pegoraro, A. Zambelli, *Chem. Abstr.* **1960**, 55, 9823i.
- [2] [2a] G. Natta, I. Pasquon, A. Zambelli, *J. Am. Chem. Soc.* **1962**, 84, 1488.
- [3] [3a] A. Razavi, J. A. Ewen, *US patent* 6184326; [3b] A. Razavi, J. A. Ewen *US patent* 4892851; [3c] A. A. Razavi, J. A. Ewen, *US patent* 5,334,677; [3d] J. A. Ewen, A. Razavi, *US patent* 5,476,914; [3e] J. A. Ewen, L. R. Jones, A. Razavi, J. J. Ferrara, *J. Am. Chem. Soc.* **1988**, 110, 6255. [3f] A. Razavi, J. J. Ferrara, *J. Organomet. Chem.* **1992**, 435, 299; [3g] Razavi, J. L. Atwood, *J. Organomet. Chem.* **1993**, 459, 117; [3h] A. Razavi, U. Thewalt, *J. Organomet. Chem.*, **1993**, 445, 111.

- [4] L. Cavallo, G. Guerra, M. Vacatello, P. Corradini, *Macromolecules* **1991**, *24*, 1784.
- [5] [5a] W. E. Piers, J. E. Bercaw, *J. Am. Chem. Soc.* **1990**, *112*, 9406; [5b] H. H. Brintzinger, H. Krauledat, *Angew. Chem., Int. Ed. Engl.* **1990**, *29*, 1412; [5c] H. H. Brintzinger, M. L. Leclerc, *J. Am. Chem. Soc.* **1995**, *117*, 1651; [5d] B. J. Burger, W. D. Cotter, E. B. Coughlin, S. T. Chascon, S. Hajela, T. A. Herzog, R. O. Koehn, J. P. Mitchell, W. E. Piers, P. J. Shapiro, J. E. Bercaw, J. E. in "Ziegler Catalyst"; G. Fink, R. H. Muelhaupt, H. H. Brintzinger, Eds; Springer verlag; Berlin, 1995. [5e] R. H. Grubbs, G. W. Goates, *Acc. Chem. Res.* **1996**, *29*, 85.
- [6] P. Cossee, E. J. Arlman, *J. Catal.* **1964**, *3*, 89. P. Cossee, The mechanism of Ziegler-Natta polymerization. II quantum chemical and crystal-chemical aspects. In: Ketly A. D, Editor. The stereochemistry of macromolecules, vol.1. New York: Marcel Dekker, **1967**, p. 145–175.
- [7] A. Razavi, L. Peters, L. Nafpliotis, D. Vereecke, K. Den Daw, *Makromol. Symp.* **1995**, *89*, 345.
- [8] A. Razavi, J. L. Atwood, *J. Organomet. Chem.* **1996**, *520*, 115.
- [9] [9a] A. Razavi, D. Vereecke, L. Peters, K. Den Daw, L. Nafpliotis, J. L. Atwood, in "Ziegler Catalysts"; Fink, G.; Muelhaupt, R.; Brintzinger, H. H., Eds.; Springer Verlag; Berlin, 1993; [9b] R. Kleinschmidt, M. Reffke, G. Fink, *Macromol. Rapid Commun.* **1999**, *20*, 284; [9c] V. Busico, R. Cipullo, G. Talarico, *Macromolecules* **1997**, *30*, 4787; [9d] A. Razavi, *C.R. Aca. Sci. Paris, Serie IIC, chimie/chemistry* **2000**, *3*, 615–625.
- [10] [10a] A. Razavi, U. Thewalt, *J. Organomet. Chem.* **2001**, *621*, 267. [10b] A. Razavi, European. Pat 96111127,5 and WO 98/02469.
- [11] [11a] A. Razavi, U. Thewalt, *J. Organomet. Chem.* **2001**, *621*, 267. [11b] V. Busico, R. Cupillo, F. Cutillo, G. Talarico, A. Razavi, *Macromol. Chem. Phys.* **2003**, *204*, 1269; [11c] A. Razavi, V. Bellia, Y. De Brauw, K. Hortmann, L. Peters, S. Sirole, S. Van Belle, V. Marine, M. Lopez, *J. Organomet. Chem.* **2003** in press; [11d] T. Shiomura, T. Asanuma, N. Inoue, *Macromol. Rapid Commun.* **1996**, *17*, 9; [11e] H. Hagihara, T. Shiono, T. Ikeda, *Macromolecules*, **1997**, *30*, 4783; [11f] H. Hagihara, T. Shiono, T. Ikeda, *Macromolecules*, **1998**, *31*, 84.
- [12] [12a] A. Razavi, V. Bellia, Y. De Brauw, K. Hortmann, M. Lambrecht, O. Miseque, L. Peters, S. Van Belle, In "Metalorganic catalysts for Synthesis and Polymerization. Ed. W. Kaminsky, Springer, Berlin (1999); [12b] A. Razavi, L. Peters, L. Nafpliotis, *J. Molecular Catalysis*, **1997**, *A. 115*, 129; [12c] H. G. Alt, M. Jung, G. Kehr, *J. Organomet. Chem.* **1998**, *562*, 153-181; [12d] D. Drago, P. S. Pergosin, A. Razavi, *Organometallics* **2000**, *19*, 1802-1805; [12e] A. K. Dash, A. Razavi, A. Mortreux, C. Lehmann, J.F. Carpentier, *Organometallics* **2002**, *21*, 3238, [12f] E. Kirlov, L. Touquet, A. Razavi, S. Kahlal, J. Y. Saillard, J. F. Carpentier, *Organometallics* **2003** submitted.
- [13] [13a] R. Leino, F. J. Gomez, A. P. Cole, R. M. Waymouth, *Macromolecules* **2001**, *34*, 2082; [13b] F. J. Gomez, R. M. Waymouth, *Macromolecules*, **2002**, *35*, 3358.
- [14] A. Kabi-satpathy, C. S. Bajgur, K. P. Reddy, J. L. Petersen, *J. Organomet. Chem.* **1989**, *364*, 105.

